

## Novel Antitrypanosomal Agents Based on Palladium Nitrofurylthiosemicarbazone Complexes: DNA and Redox Metabolism as Potential Therapeutic Targets<sup>†</sup>

Lucía Otero,<sup>⊗</sup> Marisol Vieites,<sup>⊗</sup> Lucía Boiani,<sup>‡</sup> Ana Denicola,<sup>§</sup> Carolina Rigol,<sup>||</sup> Lucía Opazo,<sup>||</sup> Claudio Olea-Azar,<sup>||</sup> Juan Diego Maya,<sup>⊥</sup> Antonio Morello,<sup>⊥</sup> R. Luise Krauth-Siegel,<sup>#</sup> Oscar E. Piro,<sup>○</sup> Eduardo Castellano,<sup>▽</sup> Mercedes González,<sup>‡</sup> Dinorah Gambino,<sup>\*⊗</sup> and Hugo Cerecetto<sup>\*‡</sup>

*Cátedra de Química Inorgánica, Departamento Estrella Campos, Facultad de Química, Departamento de Química Orgánica, Facultad de Química-Facultad de Ciencias, and Laboratorio de Físicoquímica Biológica, Facultad de Ciencias, Universidad de la República, Montevideo, Uruguay, Departamento de Química Inorgánica y Analítica, Facultad de Ciencias Químicas y Farmacéuticas, and Departamento de Farmacología Clínica y Molecular, Facultad de Medicina, Universidad de Chile, Santiago, Chile, Biochemie-Zentrum Heidelberg, Ruprecht-Karls-Universität, Heidelberg, Germany, Departamento de Física, Facultad de Ciencias Exactas, Universidad Nacional de La Plata and Instituto IFLP(CONICET), La Plata, Argentina, and Instituto de Física de São Carlos, Universidade de São Paulo, São Carlos, Brazil*

Received December 12, 2005

In the search for new therapeutic tools against American Trypanosomiasis palladium complexes with bioactive nitrofuranyl-containing thiosemicarbazones as ligands were obtained. Sixteen novel palladium (II) complexes with the formulas [PdCl<sub>2</sub>(HL)] and [Pd(L)<sub>2</sub>] were synthesized, and the crystal structure of [Pd(5-nitrofuryl-3-acroleine thiosemicarbazone)<sub>2</sub>]<sub>2</sub>·3DMSO was solved by X-ray diffraction methods. Most complexes showed higher in vitro growth inhibition activity against *Trypanosoma cruzi* than the standard drug Nifurtimox. In most cases, the activity of the ligand was maintained or even increased as a result of palladium complexation. In addition, the complexes' mode of antitrypanosomal action was investigated. Although the complexes showed strong DNA binding, all data strongly suggest that the main trypanocidal mechanism of action is the production of oxidative stress as a result of their bioreduction and extensive redox cycling. Moreover, the complexes were found to be irreversible inhibitors of trypanothione reductase.

### Introduction

Parasitic diseases represent a major health problem in Latin America. In particular, Chagas' disease (American Trypanosomiasis), caused by the protozoan parasite *Trypanosoma cruzi*, is the largest parasitic disease to burden the American continent. The morbidity and mortality associated with this disease in America are more than 1-order of magnitude higher than those caused by malaria, schistosomiasis, or leishmaniasis. Chagas' disease affects approximately 20 million people from southern United States to southern Argentina.<sup>1,2</sup> Despite the progress achieved in the study of *T. cruzi*'s<sup>a</sup> biochemistry and physiology in which several crucial enzymes for parasite survival that are absent in the host have been identified as potential new drug targets, the chemotherapy of this parasitic infection remains

undeveloped. The treatment is based on old and quite unspecific drugs that have significant activity only in the acute phase of the disease and, when associated with long-term treatments, give rise to severe side effects.<sup>3</sup> In the search for a pharmacological control of Chagas' disease, metal complexes appear to be a promising approach. The many activities of metal ions in biology have stimulated, in the past decades, the development of metal-based chemotherapeutics in different fields of medicine. Even though emphasis has been mainly placed on cancer treatment as a result of the great success of cisplatin, recent studies have also included parasitic diseases.<sup>4–7</sup> One of the successfully developed approaches has been the synthesis of complexes combining ligands bearing antitrypanosomal activity and pharmacologically active metals. The obtained derivatives could act through a dual mechanism of action combining the pharmacological properties of both the ligands and the metal.<sup>6,8–11</sup> The development of single agents that provide maximal antiprotozoal activity by acting against multiple parasitic targets could diminish host toxic effects by lowering therapeutic dose and/or circumvent the development of drug resistance.<sup>12</sup>

On the basis of this approach, we intend to develop new therapeutic tools for the treatment of Chagas' disease based on palladium complexes with bioactive 5-nitrofuryl thiosemicarbazones as ligands. Palladium was selected as the central metal atom because of the postulated metabolic similarities between tumor cells and *Trypanosoma cruzi* and its proved ability to bind DNA as the main antitumoral mechanism of action.<sup>13,14</sup> Selected 5-nitrofuryl-containing thiosemicarbazones (Scheme 1) showed higher in vitro activity against *T. cruzi* than Nifurtimox, the nitrofuranyl drug used in the past. The main mode of action of this family of compounds, as that for other nitroheterocyclic antiparasitic agents, could be related to the intracellular reduction

\* Corresponding author. Phone: +59829249739, Fax: +59829241906, E-mail: dgambino@fq.edu.uy (D.G.). Phone: +59825258618 (ext. 216), Fax: +59825250749, E-mail: hcerecetto@fq.edu.uy (H.C.).

<sup>†</sup> Part of this research is presented in the Uruguayan patent of invention: M. González, H. Cerecetto, D. Gambino, L. Otero. UR Patent No. 28563, 2004: Palladium and Platinum 5-nitrofuryl metallic complexes. Preparation Procedure and Use.

<sup>⊗</sup> Cátedra de Química Inorgánica, Universidad de la República.

<sup>‡</sup> Departamento de Química Orgánica, Universidad de la República.

<sup>§</sup> Laboratorio de Físicoquímica Biológica, Universidad de la República.

<sup>||</sup> Departamento de Química Inorgánica y Analítica, Universidad de Chile.

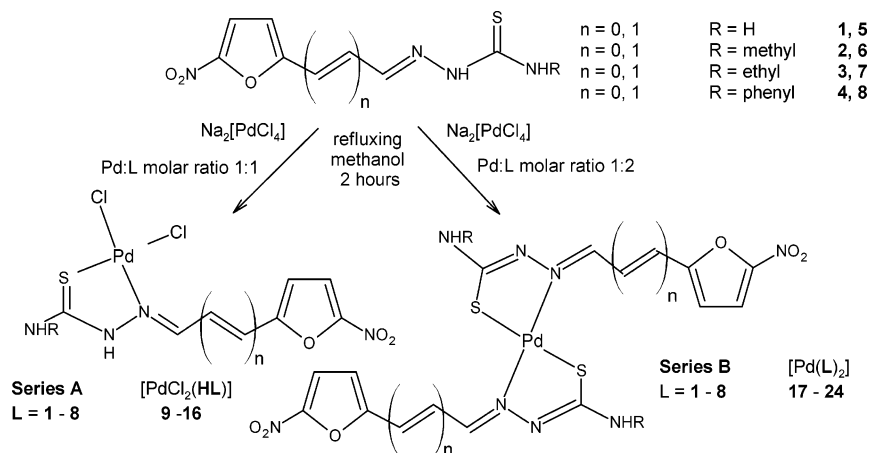
<sup>⊥</sup> Departamento de Farmacología Clínica y Molecular, Universidad de Chile.

<sup>#</sup> Ruprecht-Karls-Universität.

<sup>○</sup> Universidad Nacional de La Plata and Instituto IFLP(CONICET).

<sup>▽</sup> Universidade de São Paulo.

<sup>a</sup> Abbreviations: *T. cruzi*, *Trypanosoma cruzi*; ROS, reactive oxygen species; TR, trypanothione reductase; TS<sub>2</sub>, trypanothione disulfide; T(SH)<sub>2</sub>, trypanothione; *v*, stretching; HETCOR, heteronuclear correlation experiments; Nfx, Nifurtimox; SCE, saturated calomel electrode; ESR, electronic spin resonance; DMPO, 5,5 dimethyl-1-pyrroline-*N*-oxide; CT DNA, calf thymus DNA; TBAP, tetrabutylammonium perchlorate; PGI, percentage growth inhibition.

**Scheme 1.** Synthesis of Palladium Complexes of Selected 5-Nitrofuryl-Containing Thiosemicarbazones

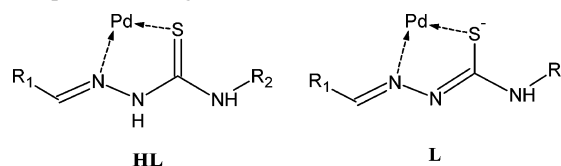
of the nitro moiety followed by redox cycling, yielding reactive oxygen species (ROS) known to cause cellular damage.<sup>15,16</sup>

In addition, many nitrofuran drugs have proved to be subversive substrates of the parasite specific flavoenzyme trypanothione reductase (TR).<sup>17</sup> However, a group of platinum complexes have been shown to be irreversible inhibitors of TR.<sup>18,19</sup> In trypanosomes, the nearly ubiquitous glutathione/glutathione reductase system is replaced by trypanothione and trypanothione reductase. One of the essential roles of TR is the maintenance of a reducing intracellular milieu. Trypanosomes depend on TR, which keeps their main thiols, bisglutathionyl-spermidine (trypanothione, T(SH)<sub>2</sub>) and monoglutathionylspermidine (Gsp), in the thiol state:  $\text{TS}_2 + \text{NADPH} + \text{H}^+ \rightarrow \text{T}(\text{SH})_2 + \text{NADP}^+$ . The absence of trypanothione in the mammalian host and the uniqueness of the parasite thiol metabolism together with the essential role of TR in the defense of trypanosomatids against oxidative stress render trypanothione reductase an attractive drug target.<sup>20-22</sup>

In this work, we describe the development of novel palladium complexes with 5-nitrofuryl containing thiosemicarbazones as ligands that could act against *T. cruzi*'s redox metabolism and DNA. Two series of complexes of the formulas  $[\text{PdCl}_2(\text{HL})]$  and  $[\text{Pd}(\text{L})_2]$  (Scheme 1), where HL is the neutral thiosemicarbazones shown in Scheme 1 and L, the monodeprotonated forms, were synthesized and characterized. The in vitro activity against *T. cruzi* was evaluated, and some aspects related to their mechanism of action were studied. The intracellular production of free radicals by the complexes was studied by electron paramagnetic resonance (EPR) spectroscopy. Oxygen uptake was measured in the parasites to evaluate the possible induction of redox cycling by the complexes. In addition, the ability of the palladium compounds to inhibit the enzyme TR and interact with DNA was studied.

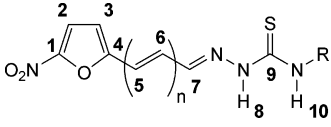
**Results and Discussion**

**Chemistry. Synthesis.** By reacting  $\text{Na}_2[\text{PdCl}_4]$  or  $[\text{PdCl}_2(\text{DMSO})_2]$  with each of the thiosemicarbazones **1-8** shown in Scheme 1, two series of palladium compounds, **9-24**, were obtained. Complexes of the formulas  $[\text{PdCl}_2(\text{HL})]$  (series A, **9-16**, Scheme 1) were synthesized using a 1:1 palladium to ligand molar ratio. If a 1:2 palladium to ligand molar ratio was used, complexes of the formulas  $[\text{Pd}(\text{L})_2]$  (series B, **17-24**, Scheme 1) were obtained. In both cases, N,S bidentate coordination was observed (Scheme 1). The compounds were isolated in high purity and good yields. All of them are nonconducting compounds, and the analytical results are in agreement with the proposed formula.

**Scheme 2.** Thiosemicarbazone Acting as a Neutral (HL) or Monodeprotonated Ligand (L)

**FT-IR and Raman Spectroscopies.** Significant vibration bands of the metal complexes, useful for determining the ligand's mode of coordination, could be tentatively assigned. Raman spectra allow a better assignment of the infrared bands. After coordination, the  $\nu(\text{C}=\text{N})$  IR bands of the thiosemicarbazone free ligands, at approximately  $1500-1600 \text{ cm}^{-1}$ , shift to higher frequencies. In addition,  $\nu(\text{C}=\text{S})$  IR bands, at approximately  $820-840 \text{ cm}^{-1}$ , shift to lower frequencies. These modifications are consistent with the bidentate coordination of the thiosemicarbazone ligands through the thiocarbonylic sulfur and the azomethynic nitrogen.<sup>23-27</sup> The  $\nu(\text{NH})$  IR band, at approximately  $3120-3150 \text{ cm}^{-1}$ , is present in all series A complexes indicating that the ligand is nondeprotonated in these complexes. In contrast, the  $\nu(\text{NH})$  band is not observed in all series B complexes because of deprotonation of the ligands. In addition, the frequency shift of the  $\nu(\text{C}=\text{S})$  IR band of all series B complexes is larger ( $60-120 \text{ cm}^{-1}$ ) than that observed in the series A complexes ( $10-50 \text{ cm}^{-1}$ ) because of the lowering of the C-S bond order owing to deprotonation (Scheme 2).

**NMR Spectroscopy.** The low solubility of complexes from series B and some derivatives from series A prevented the acquiring of the complete series of <sup>1</sup>H- and <sup>13</sup>C NMR spectra. The NMR experiments performed confirm the structures of the synthesized complexes, and the results are in agreement with those of the other spectroscopies. The <sup>1</sup>H NMR experiments show narrow signals, typical for Pd(II) square planar diamagnetic complexes. HETCOR experiments allowed us to assign all signals of the free ligands and the investigated complexes. <sup>1</sup>H NMR integrations and signal multiplicities are in agreement with the proposed formula. Some of the obtained results are shown in Table 1. The attached figure shows the numbering scheme of the free ligands mentioned in the Table and the text. The complexes show similar <sup>1</sup>H and <sup>13</sup>C chemical shifts of the nitrofurylthiosemicarbazone common portion of their molecules. When the ligand is coordinated, the effect of the metal is apparent for the protons that are located close to the coordinating atoms, the azomethynic nitrogen, and the thiocarbonylic sulfur (see the values of  $\Delta\delta$ , Table 1). The presence of a signal corresponding to proton 8 is in accordance with the coordination

**Table 1.** <sup>1</sup>H- and Selected <sup>13</sup>C NMR Chemical Shift Values ( $\delta$ ) of L and [PdCl<sub>2</sub>(HL)] at 303 K


<sup>1</sup> H NMR	<i>(n</i> = 0, R = Me)		<i>(n</i> = 0, R = Et)		<i>(n</i> = 1, R = Me)		<i>(n</i> = 1, R = Et)		$\Delta\delta^a$				
	H	$\delta_{\text{ligand } 2^b}$	$\delta_{\text{complex } 10^b}$	$\delta_{\text{ligand } 3^b}$	$\delta_{\text{complex } 11^b}$	$\delta_{\text{ligand } 6^b}$	$\delta_{\text{complex } 14^c}$	$\delta_{\text{ligand } 7^b}$	$\delta_{\text{complex } 15^d}$	$\Delta\delta_2$	$\Delta\delta_3$	$\Delta\delta_6$	$\Delta\delta_7$
<b>2</b>		7.79	7.79	7.79	7.79	7.72	7.63	7.72	7.62	0.00	0.00	0.09	-0.10
<b>3</b>		7.30	7.53	7.31	7.51	6.98	7.12	7.00	7.05	0.23	0.20	0.14	0.05
<b>5</b>						7.00	7.20	7.00	7.23			0.20	0.23
<b>6</b>						7.00	7.77	7.00	7.60			0.77	0.60
<b>7</b>		7.98	8.21	7.98	8.21	7.87	8.16	7.87	8.49	0.23	0.23	0.29	0.62
<b>8</b>		11.87	9.07	11.82	9.18	11.61	8.40	11.57	10.00	-2.80	-2.64	-3.21	-1.57
<b>10</b>		8.52	8.27	8.54	8.30	8.46	7.30	8.47	7.90	-0.25	-0.22	-1.16	-0.57
<b>11</b>		3.03	2.87	3.60	3.32	2.98	2.96	3.55	3.53	-0.16	-0.28	-0.02	-0.02
<b>12</b>				1.07	1.18			1.12	0.90		0.11		-0.22

<sup>13</sup> C NMR	<i>(n</i> = 0, R = Me)		<i>(n</i> = 0, R = Et)		<i>(n</i> = 1, R = Me)		$\Delta\delta^a$			
	C	$\delta_{\text{ligand } 2^b}$	$\delta_{\text{complex } 10^b}$	$\delta_{\text{ligand } 3^b}$	$\delta_{\text{complex } 11^b}$	$\delta_{\text{ligand } 6^b}$	$\delta_{\text{complex } 14^c}$	$\Delta\delta_2$	$\Delta\delta_3$	$\Delta\delta_6$
<b>7</b>		130.21	138.01	130.29	137.91	142.31	152.86	7.80	7.62	10.55
<b>9</b>		178.63	174.41	177.68	173.88	178.59		-4.22	-3.80	-

<sup>a</sup>  $\Delta\delta = (\delta_{\text{complex}} - \delta_{\text{ligand}})$ . <sup>b</sup> DMSO-*d*<sub>6</sub>. <sup>c</sup> Acetone-*d*<sub>6</sub>:DMSO-*d*<sub>6</sub> (9:1). <sup>d</sup> Acetone-*d*<sub>6</sub>. <sup>e</sup> Not observed because of solubility problems.

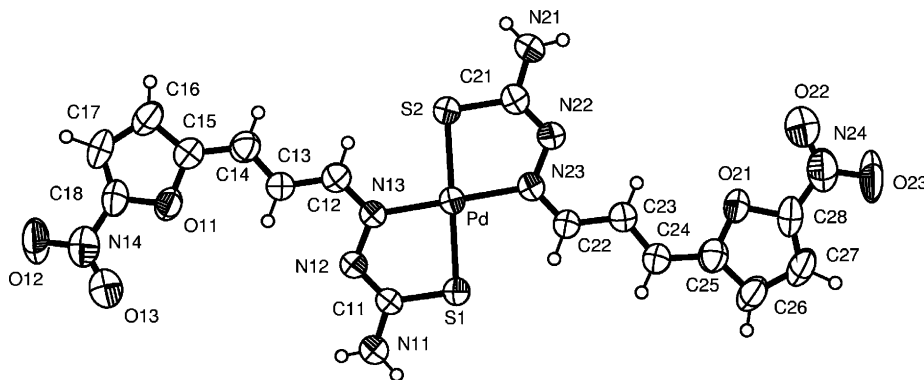
**Table 2.** Bond Lengths (Å) and Angles (°) around the Palladium(II) Atom in [Pd(L5)<sub>2</sub>] $\cdot$ 3DMSO

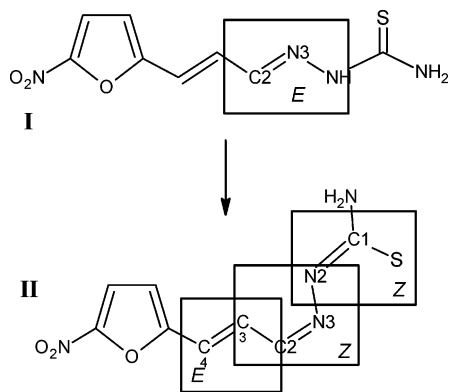
bond distances	
Pd–N(23)	2.027(6)
Pd–N(13)	2.027(6)
Pd–S(2)	2.283(2)
Pd–S(1)	2.298(2)
bond angles	
N(23)–Pd–N(13)	179.2(2)
N(23)–Pd–S(2)	83.3(2)
N(13)–Pd–S(2)	96.5(2)
N(23)–Pd–S(1)	97.1(2)
N(13)–Pd–S(1)	83.1(2)
S(2)–Pd–S(1)	178.6(1)

of the ligands in a nondeprotonated form. Furthermore, the largest  $\Delta\delta$  values are observed for this proton. Upon coordination, the most distinguishing feature of the <sup>13</sup>C NMR spectra is the change in the chemical shifts of the carbons numbered 7 and 9 that are located near the coordinating atoms.

**Crystal Structure of Derivative 21.** Red single crystals, suitable for X-ray diffraction methods, of derivative **21** were obtained by slow diffusion of water into a DMSO solution of the studied compound. The compound is obtained with DMSO crystallization molecules and can be described by the chemical formula [Pd(L5)<sub>2</sub>] $\cdot$ 3DMSO. Relevant intramolecular bond distances and angles around the metal ion are shown in Table 2.

Figure 1 is an ORTEP<sup>28</sup> drawing of the molecule showing the labeling scheme of the non-H atoms and their displacement ellipsoids at the 50% probability level. The X-ray diffraction study shows that the complex (Pd(L5)<sub>2</sub>) consists of discrete monomeric molecules. The Pd(II) ion is trans coordinated by two nearly coplanar deprotonated thiosemicarbazone molecules (rms deviation of atoms from the least-squares plane of 0.21 Å) acting as bidentate ligands through their sulfur (Pd–S bond distances of 2.258(2) and 2.283(2) Å) and azomethynic nitrogen (both Pd–N distances equal to 2.027(6) Å) atoms. These bond distances are quite similar to those observed in other palladium thiosemicarbazone complexes.<sup>25,29,30</sup> In particular, other reported complexes of the formula *trans*-PdL<sub>2</sub> showed almost identical Pd–S and Pd–N bond distances to those obtained in this work (2.286(2) and 2.028(7) Å, respectively).<sup>31</sup> Intraligand bond distances are in accordance with the high electronic delocalization of the deprotonated thiosemicarbazone ligands. C–S bond distances (1.743(7) and 1.730(8) Å) correspond to a single bond character, whereas C(1)–N(2) bond distances (1.315(11) and 1.302(10) Å) account for the double bond character of these bonds.<sup>25,30–32</sup> Both coordinated thiosemicarbazones present a spatial distribution *Z, Z, E* around the C(1)–N(2), N(3)–C(2) and C(3)–C(4) bonds (numbering according to Scheme 3). The *Z* distribution around the C(1)–N(2) bond is imperative for N,S bidentate coordination. In addition, as a consequence of the

**Figure 1.** ORTEP drawing of [Pd(L5)<sub>2</sub>] $\cdot$ 3DMSO. Carbon atoms are denoted by crossed ellipsoids, whereas palladium, sulfur, oxygen, and nitrogen atoms are indicated by hatched ones. DMSO crystallization molecules are omitted for clarity.

**Scheme 3.** Spatial Distribution of the Thiosemicarbazone Ligand **5** before (**I**) and after (**II**) Coordination to Palladium**Table 3.** In Vitro Biological Activity of Both Series of Pd Complexes

compd	rPGI <sub>Nfx</sub> <sup>a</sup>	IC <sub>50</sub> (μM) <sup>b</sup>	compd	rPGI <sub>Nfx</sub> <sup>a</sup>	IC <sub>50</sub> (μM) <sup>b</sup>
<b>1</b>	1.5 <sup>c</sup>	2.7	<b>5</b>	1.6 <sup>c</sup>	3.5
<b>9</b> , [PdCl <sub>2</sub> (HL1)]	1.3	2.4	<b>13</b> , [PdCl <sub>2</sub> (HL5)]	1.2	6.4
<b>17</b> , [Pd(L1) <sub>2</sub> ]	1.5	4.5	<b>21</b> , [Pd(L5) <sub>2</sub> ]	1.0	4.3
<b>2</b>	1.1 <sup>c</sup>	5.0	<b>6</b>	1.3 <sup>c</sup>	4.5
<b>10</b> , PdCl <sub>2</sub> (HL2)]	1.1	4.3	<b>14</b> , [PdCl <sub>2</sub> (HL6)]	1.4	2.7
<b>18</b> , [Pd(L2) <sub>2</sub> ]	0.9	4.7	<b>22</b> , [Pd(L6) <sub>2</sub> ]	1.5	4.3
<b>3</b>	1.1 <sup>c</sup>	4.9	<b>7</b>	1.6 <sup>c</sup>	4.1
<b>11</b> , [PdCl <sub>2</sub> (HL3)]	0.8	5.9	<b>15</b> , [PdCl <sub>2</sub> (HL7)]	1.4	2.4
<b>19</b> , [Pd(L3) <sub>2</sub> ]	0.3	ND	<b>23</b> , [Pd(L7) <sub>2</sub> ]	1.4	5.2
<b>4</b>	0.3 <sup>c</sup>	ND	<b>8</b>	1.7 <sup>c</sup>	3.6
<b>12</b> , [PdCl <sub>2</sub> (HL4)]	0.1	ND	<b>16</b> , [PdCl <sub>2</sub> (HL8)]	0	ND
<b>20</b> , [Pd(L4) <sub>2</sub> ]	0	ND	<b>24</b> , [Pd(L8) <sub>2</sub> ]	0	ND

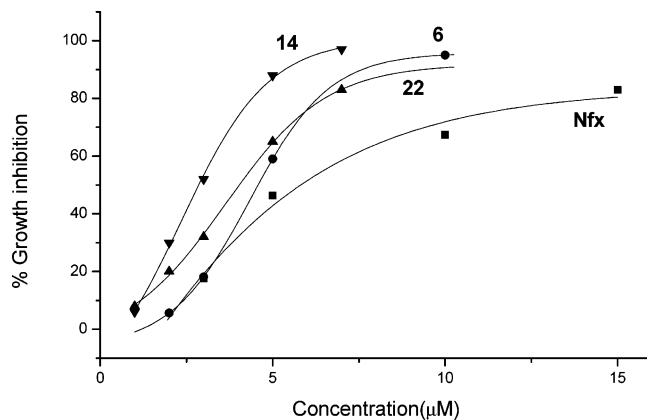
<sup>a</sup> rPGI<sub>Nfx</sub>: ratio of percentage of growth inhibition of *T. cruzi* epimastigote cells at 5 μM with respect to Nfx (PGI of Nfx was taken as 1.0). PGI: percentage of growth inhibition at 5 μM. <sup>b</sup> IC<sub>50</sub>: 50% inhibitory concentration. <sup>c</sup> Reference<sup>16</sup> ND: not determined.

formation of the five-membered chelate ring, the thiosemicarbazone ligands suffer a stereochemical change around the C(2)=N(3) bond, relative to the free ligand structure. Therefore, although the free ligand exists as the isomeric form *E* around C(2)=N(3) bond, X-ray diffraction studies show that upon coordination to palladium it adopts the isomeric form *Z*.<sup>33</sup> The planar complexes are arranged in the lattice parallel to one another conforming a layered structure. Each layer is stabilized through an intermolecular hydrogen bond net that involves both hydrogen atoms from the terminal thioamide groups and the oxygen atoms of two crystallization DMSO molecules that act as bridges between two complexes.

**Biology. Anti *T. cruzi* Activity.** Table 3 shows the effect of the palladium complexes and the corresponding free ligands<sup>16</sup> on the growth of the epimastigote form of *T. cruzi* at 5 μM at day 5 of exposure. Most of the complexes proved to be as active as the ligands, and they were up to 1.7-fold more active than Nfx at this dosage. Complexes with ligands **4** and **8** did not inhibit *T. cruzi* growth under the assayed conditions. For the most active complexes, dose–response curves were recorded, and the IC<sub>50</sub> values were calculated (Table 3). According to the IC<sub>50</sub> values, **9**, **14**, and **15** were the most active complexes. Although, the IC<sub>50</sub> values were quite similar for each ligand and its complexes, the following trend could be observed: series A complex [PdCl<sub>2</sub>(HL)] > free ligand > series B complex [Pd(L)<sub>2</sub>].

As an example, the dose response curves for ligand **6** and its palladium complexes **14** and **22** are shown in Figure 2.

**Effect on Parasite Redox Metabolism.** To elucidate if the antiparasitic activity of the new compounds correlates with an

**Figure 2.** Dose–response curves for **6**, **14**, and **22**. Percent growth inhibition was determined on the 5th day of culture. Nfx is included for comparison.**Table 4.** Potentials (V) vs SCE (Saturated Calomel Electrode) of the Nitro Group Redox Couple for the Pd Complexes and the Free Ligands

compd	<i>E</i> <sub>pc</sub> (V) <sup>a</sup>	<i>E</i> <sub>pa</sub> (V) <sup>b</sup>	<i>E</i> <sub>1/2</sub> (V) <sup>c</sup>	compd	<i>E</i> <sub>pc</sub> (V) <sup>a</sup>	<i>E</i> <sub>pa</sub> (V) <sup>b</sup>	<i>E</i> <sub>1/2</sub> (V) <sup>c</sup>
<b>1</b>	−0.84	−0.75	−0.80	<b>5</b>	−0.84	−0.72	−0.78
<b>9</b>	−0.83	−0.70	−0.76	<b>15</b>	−0.78	−0.68	−0.73
<b>17</b>	−0.82	−0.72	−0.76	<b>23</b>	−0.77	−0.71	−0.74
<b>2</b>	−0.79	−0.71	−0.75	<b>6</b>	−0.79	−0.70	−0.74
<b>10</b>	−0.82	−0.70	−0.76	<b>14</b>	−0.81	−0.71	−0.76
<b>18</b>	−0.84	−0.75	−0.80	<b>22</b>	−0.80	−0.73	−0.76
<b>3</b>	−0.79	−0.71	−0.75	<b>7</b>	−0.79	−0.71	−0.75
<b>11</b>	−0.71	−0.70	−0.70	<b>15</b>	−0.84	−0.73	−0.78
<b>19</b>	−0.79	−0.69	−0.74	<b>23</b>	−0.89	−0.64	−0.76
<b>4</b>	−0.78	−0.70	−0.74	<b>8</b>	−0.77	−0.70	−0.74
<b>12</b>	−0.74	−0.69	−0.72	<b>16</b>	−0.81	−0.76	−0.78
<b>20</b>	−0.73	−0.69	−0.71	<b>24</b>	−0.81	−0.75	−0.78
Nifurtimox	−0.91	−0.85	−0.88				

<sup>a</sup> *E*<sub>pc</sub> = cathodic peak potential. <sup>b</sup> *E*<sub>pa</sub> = anodic peak potential. <sup>c</sup> *E*<sub>1/2</sub> = (*E*<sub>pc</sub> + *E*<sub>pa</sub>)/2.

oxidative stress-mediated mechanism of action, the electrochemical behavior of the complexes as well as the production of free radicals into the parasite and the effect of the compounds on the parasitic oxygen consumption was determined.

**Electrochemical Behavior.** Voltammetric studies in DMSO were performed to determine the effect of palladium complexation on the peak potential of the nitro moiety. Figure 3 shows a typical voltammogram for **6** and corresponding palladium complexes **14** and **22**. Similar reduction behavior was observed for all palladium complexes, and it is also similar to that previously reported for the thiosemicarbazone ligands.<sup>34</sup> When the potential was scanned in a negative direction, at all scan rates investigated, it was observed as a peak near −0.8 V versus SCE, which corresponds to the reduction of the nitro group. Table 4 lists the values of the voltammetric peaks corresponding to the nitro moiety. These potentials slightly changed as a consequence of palladium complexation ( $\Delta V_{\text{max.}} = \pm 0.05$  V). However, it should be stated that all studied compounds exhibited higher *E*<sub>1/2</sub> values than Nfx (−0.88 V), showing a higher capacity to be reduced and, therefore, a better ability to generate radical species that could be toxic for the parasite.

**Capacity of Derivatives to Generate Free Radical Species into *T. cruzi*.** The proposed bioreduction of the palladium complexes involves the production of free radical species in the parasite. EPR experiments were performed in the presence of 5,5-dimethyl-1-pyrroline-*N*-oxide (DMPO) to trap free radical species having short half-lives. Well resolved 10 line-spectra were observed when *T. cruzi* were incubated with active

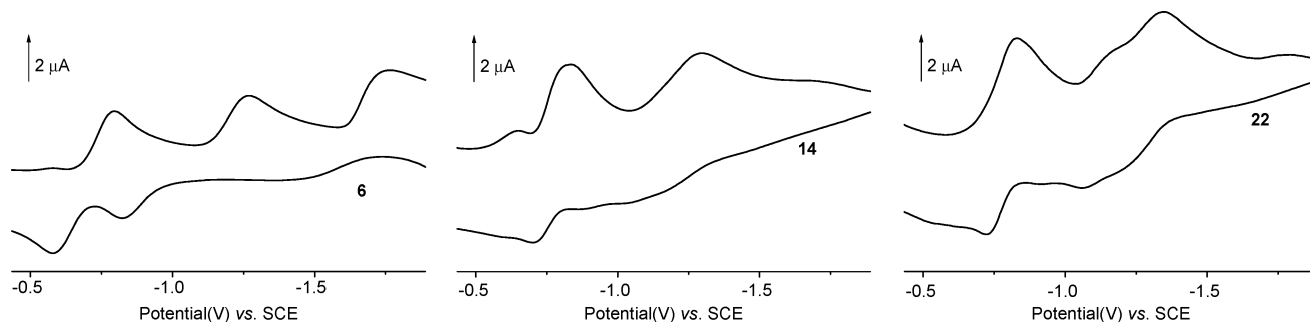


**Figure 3.** Cyclic voltammogram of 1 mM DMSO solutions of ligand **6** and complexes **14** and **22**, 0.1 M TBAP, and 2000 mV/s.

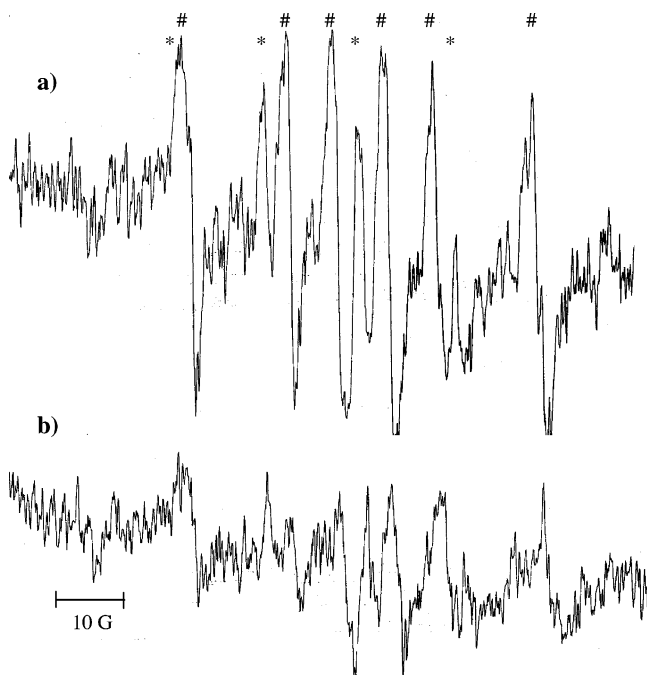


**Figure 4.** EPR spectra obtained after 5 min of incubation of **14** (a) and **22** (b) (1 mM) with intact *T. cruzi* epimastigotes (Brener strain,  $600 \times 10^6$  cells/mL), NADPH (1 mM), EDTA (1 mM), and DMPO (100 mM). (\*) DMPO–OH spin adduct, (#) DMPO–nitro complex spin adduct.

palladium complexes (Figure 4). The EPR signals were consistent with the trapping of both the hydroxyl radical and the nitroheterocyclic radical of the complexes. Observed hyperfine constants for the DMPO–OH spin adduct ( $a_N = a_H$  around 15.3 G) and the DMPO–nitro complex spin adducts ( $a_N$  around 23.4 G and  $a_H$  around 15.5 G) are in agreement with the splitting constants of other DMPO–OH adducts and nitrogen-centered radicals trapped by DMPO.<sup>35–39</sup> There was a good correlation between the EPR signal intensities, and thus the radical species concentration, with the observed *T. cruzi* IC<sub>50</sub> values. As described above, complexes with ligands **4** and **8** showed no inhibition of *T. cruzi* growth, and also, no EPR signals were observed. Moreover, for series A complexes, the most active derivatives, the intensities of the EPR signals were higher than those for the series B complexes, as shown in Figure 4 for **14** (series A) and **22** (series B). This correlation is also found for complexes, such as those of **5**, whose activity tendency was the opposite (spectra not shown). These results support the idea that the main trypanocidal effect of the palladium compounds studied here occurs through a mechanism involving the production of oxygen radical species.

**Oxygen Uptake.** The involvement of the palladium complexes in redox cycling processes should increase the parasite oxygen consumption. Thus, oxygen uptake, with and without

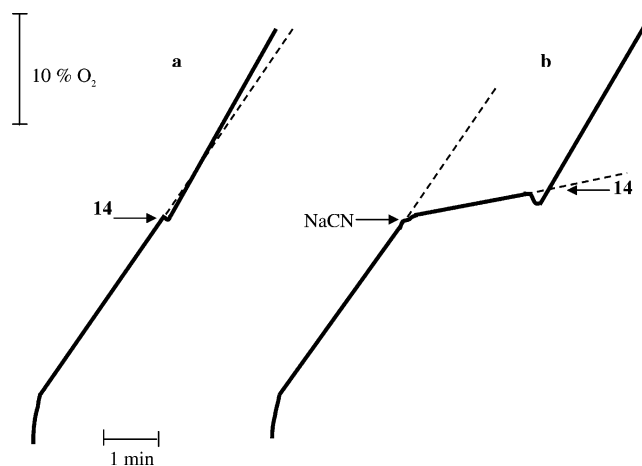


**Figure 5.** (a) Effect of compound **14** (150  $\mu$ M) on the parasite oxygen consumption related to that of the control (---). (b) Effect of compound **14** (600  $\mu$ M) on the parasite oxygen consumption after inhibition of mitochondrial respiration using (0.3 mM) cyanide (---). The complex seems to restore mitochondrial respiration (see text).

**Table 5.** Effect of the Addition of Pd Complexes (**9–24**) on the Oxygen Uptake by *T. cruzi* Epimastigotes (Tulahuen Strain)

compd	increase in oxygen uptake <sup>a</sup> (%)	redox cycling <sup>b</sup> (%)
<b>9</b> , [PdCl <sub>2</sub> (HL1)]	5	
<b>10</b> , [PdCl <sub>2</sub> (HL2)]	20	
<b>13</b> , [PdCl <sub>2</sub> (HL5)]	12	
<b>14</b> , [PdCl <sub>2</sub> (HL6)]	7	
<b>22</b> , [Pd(L6) <sub>2</sub> ]	10	50
<b>15</b> , [PdCl <sub>2</sub> (HL7)]	7	
<b>23</b> , [Pd(L7) <sub>2</sub> ]	0	160
<b>16</b> , [PdCl <sub>2</sub> (HL8)]	13	

<sup>a</sup> Percent increase of oxygen consumption after the addition of 150  $\mu$ M of compounds with respect to that of the control (no added compound).

<sup>b</sup> Percent increase of oxygen consumption after the addition of 600  $\mu$ M of compound with respect to the respiration inhibited with 0.3 mM cyanide.

the inhibition of *T. cruzi* respiration with cyanide, was measured for complexes **9–24**. The effect of complex **14** on *T. cruzi* epimastigote respiration is shown in Figure 5. Most of the compounds increased oxygen consumption, and the effect was more obvious after inhibition of the parasite mitochondrial respiration (Table 5). These results are in accordance with the detection of free radical species in the EPR experiments and with a bioreductive and redox cycling mechanism of action as previously reported for Nifurtimox and other nitrofurans derivatives.<sup>40</sup> It should be noted that to validate a correlation between growth inhibition and intraparasitic redox cycling (Experimental Section), fairly concentrated solutions of compounds are needed for the latter experiments. Thus, respiration and redox cycling values were not determined for some of the palladium complexes

**Table 6.** Inhibition of *T. cruzi* Trypanothione Reductase by **7**, **9**, **13**, **15**, and **23**<sup>a</sup>

compd	inhibitor TS <sub>2</sub>		volume activity (U/mL)	inhibition (%)
	concentration in the assay (μM)			
<b>7</b>	0 <sup>b</sup>	105	3.68	
	40	105	2.09	43
	80	105	1.66	57
<b>9</b> , [PdCl <sub>2</sub> (HL1)] <sup>c</sup>	0 <sup>b</sup>	105	2.80	
	4	105	1.25	55
	8	105	0.82	71
<b>13</b> , [PdCl <sub>2</sub> (HL5)] <sup>c</sup>	0 <sup>b</sup>	93	2.65	
	4	93	2.00	25
	10	93	1.32	50
<b>15</b> , [PdCl <sub>2</sub> (HL7)] <sup>c</sup>	0 <sup>b</sup>	105	3.05	
	1	105	2.64	13
	5	105	2.07	32
<b>23</b> , [Pd(L7) <sub>2</sub> ] <sup>c</sup>	0 <sup>b</sup>	105	2.63	
	8	105	2.25	14

<sup>a</sup> The kinetics were carried out as described under Experimental Procedures. <sup>b</sup> The control assays contained the respective amount of DMSO. <sup>c</sup> At higher concentrations, either the Pd-complexes caused too high of an absorption at 340 nm or they were not completely soluble. The values are the mean of at least two independent measurements that differed by less than 10%.

because of their poor solubility. The insolubility could also be the reason for the observed independence of the respiration values with complex concentration. However, redox cycling values could not be determined for series A complexes because they seem to restore mitochondrial respiration in the presence of cyanide (Figure 5). The cyanide anion acting as ligand for palladium through chloride substitution reactions could be the reason for the disappearance of the cyanide effect on parasite respiration after the addition of series A complexes.

**Inhibition of *T. cruzi* Trypanothione Reductase.** Several of the new Pd complexes were studied as inhibitors of *T. cruzi* TR. The three [PdCl<sub>2</sub>(HL)] complexes selected included ligands with and without substituent R and *n* = 0 or 1 (Scheme 1). Most of the [Pd(L)<sub>2</sub>] complexes could not be studied because of their low solubility in the reaction buffer. The [PdCl<sub>2</sub>(HL)] complexes proved to be efficient inhibitors of trypanothione reductase. Low micromolar concentrations of complexes **9** and **13** caused 50% inhibition in the presence of 100 μM TS<sub>2</sub>, which corresponds to a substrate concentration of 6 × *K<sub>m</sub>* (Table 6). In comparison, free ligand **7** was only a weak inhibitor. For complex **9**, the type of reversible inhibition was determined. The complex shows uncompetitive inhibition versus TS<sub>2</sub>. In a second series of kinetics, **9**, **13**, and **15** were studied for their ability to irreversibly inactivate the parasite enzyme. As shown in Table 7, the incubation of TR with the Pd complexes in the presence of NADPH caused a time-dependent inactivation of the enzyme. Free ligand **7** did not result in any inhibition under these conditions. In the absence of NADPH, the complexes cause only very weak inhibition. These data are in accordance with the 2-electron reduced enzyme, where the redox active Cys52–Cys57 couple is present as dithiol, being the reacting protein species. Reversible inhibition is not detectable under the conditions applied. Extensive dialysis of the modified protein did not result in an increase of the remaining TR activity, and even treatment of the dialyzed protein samples with excess thiol did not recover the enzyme activity. Taken together, the Pd complexes react with *T. cruzi* TR most probably by specifically modifying Cys52 in the active site of the reduced enzyme. In comparison to purely competitive ligands, irreversible inhibitors may be effective at much lower concentrations, and in addition,

**Table 7.** Time-Dependent Inactivation of Reduced *T. cruzi* Trypanothione Reductase by **7**, **9**, **13**, and **15**

reaction mixture	preincubation time (min)				
	0	30	60	120	150
volume activity (U/mL)					
NADPH, TR (control 1)	3.00	3.19	3.06		
<b>7</b> (120 μM), TR (control 2)	3.00	2.80	3.12		
NADPH, <b>7</b> (120 μM), TR	3.00	3.09	2.96		
NADPH, TR (control 1)	3.38	3.87	3.38		3.22
<b>9</b> (12 μM), TR (control 2)	3.00	3.19	3.16		3.06
NADPH, <b>9</b> (12 μM), TR	2.03	1.16	0.84		0.61
NADPH, TR (control 1)	3.54	3.19	3.22	3.22	
<b>13</b> (20 μM), TR (control 2)	2.90	2.96	2.96	2.90	
NADPH, <b>13</b> (20 μM), TR	2.38	1.03	0.54	0.25	
NADPH, TR (control 1)	3.54	3.19	3.22	3.22	
<b>15</b> (40 μM), TR (control 2)	2.64	2.74	2.54	2.58	
NADPH, <b>15</b> (40 μM), TR	1.93	0.55	0.26	0.19	

**Table 8.** Interaction of the Pd Complexes with CT DNA after 96 Hours of Incubation at 37 °C

compd	nmol Pd/mg of DNA	metal/base <sup>a</sup>	base/metal
<b>9</b> , [PdCl <sub>2</sub> (HL1)]	419	0.138	7
<b>17</b> , [Pd(L1) <sub>2</sub> ]	275	0.091	11
<b>10</b> , [PdCl <sub>2</sub> (HL2)]	528	0.174	6
<b>18</b> , [Pd(L2) <sub>2</sub> ]	393	0.130	8
<b>11</b> , [PdCl <sub>2</sub> (HL3)]	568	0.188	5
<b>19</b> , [Pd(L3) <sub>2</sub> ]	402	0.133	8
<b>12</b> , [PdCl <sub>2</sub> (HL4)]	539	0.178	6
<b>13</b> , [PdCl <sub>2</sub> (HL5)]	518	0.171	6
<b>14</b> , [PdCl <sub>2</sub> (HL6)]	519	0.171	6
<b>15</b> , [PdCl <sub>2</sub> (HL7)]	440	0.145	7
<b>16</b> , [PdCl <sub>2</sub> (HL8)]	459	0.151	7

<sup>a</sup> Palladium (mol) per DNA base (mol).

the accumulation of the substrate due to a blockage of the pathway cannot overcome inhibition. This renders irreversible inhibitors of the parasite enzyme promising drug candidates.

**Interaction with Calf Thymus DNA.** The binding of the Pd complexes to DNA was studied by combining atomic absorption determinations (for the metal) and electronic absorption measurements for DNA quantification. A complete study of all [Pd(L)<sub>2</sub>] complexes could not be performed because of their low solubility in the assayed conditions. The new complexes are excellent binding agents for CT DNA (Table 8). The observed palladium DNA binding levels were higher than those of known antitumor metal complexes.<sup>14</sup> For series A [PdCl<sub>2</sub>(HL)] complexes, DNA binding levels were higher than those for series B [Pd(L)<sub>2</sub>] complexes. The former, having labile chloride ligands probably interact with DNA through a mechanism similar to that previously reported for cisplatin, becoming activated through aquation and reaction with nucleophilic DNA bases.<sup>41</sup> The latter complexes cannot act in this way but, being planar, they may intercalate DNA. However, series A complexes also contain a planar motive so intercalation could also be possible in this case. For a given series, the binding levels were almost independent of the nature of the thiosemicarbazone ligand. It is interesting to note that no correlation between *T. cruzi* growth inhibition and DNA binding was observed.

## Conclusions

Sixteen new palladium complexes of the formula [PdCl<sub>2</sub>(HL)] and [Pd(L)<sub>2</sub>] with nitrofuranyl-containing thiosemicarbazones as ligands were synthesized and fully characterized. The complexes, except those with **4** and **8** as ligands, were, in vitro, more active than Nifurtimox against *T. cruzi*. In most cases, the biological activity of the respective ligand was maintained

or increased as a result of palladium complexation. Even though all obtained complexes bind DNA, their main toxic effect on the parasite seems to be related to redox metabolism. All performed experiments strongly suggest that the main mechanism underlying the trypanocidal activity of the complexes is the production of oxidative stress as a result of their bioreduction and extensive redox cycling. Moreover, the irreversible inhibition of trypanothione reductase should enhance the oxidative stress in the parasite. The promising results obtained herein make these novel palladium complexes good candidates for further *in vivo* studies.

## Experimental Procedures

**Materials and Methods.** All common laboratory chemicals were purchased from commercial sources and used without further purification.  $\text{Na}_2[\text{PdCl}_4]$  was commercially available.  $[\text{Pd}^{\text{II}}\text{Cl}_2(\text{DMSO})_2]$  was prepared according to literature procedures.<sup>42</sup> All thiosemicarbazone ligands were synthesized using the methodology previously reported.<sup>16</sup> C, H, N, and S analyses were performed with a Carlo Erba Model EA1108 elemental analyzer. Conductometric measurements were performed at 25 °C in  $10^{-3}$  M dimethylformamide (DMF) solutions using a Conductivity Meter 4310 Jenway.<sup>43</sup> FTIR spectra (4000–400 and 500–200  $\text{cm}^{-1}$ ) of the complexes, and the free ligands were measured either as KBr or CsI pellets with a Bomen FTIR model M102 instrument. Raman spectra were scanned with the FRA 106 accessory of a Bruker IF 66 FTIR spectrophotometer. The 1064 nm radiation of a Nd:YAG laser was used for excitation, and 50–60 scans were routinely accumulated. Electronic spectra were recorded on a Spectronic 3000 spectrophotometer.  $^1\text{H}$  NMR and  $^{13}\text{C}$  NMR spectra of the free ligands and of the complexes were recorded on a Bruker DPX-400 instrument (at 400 and 100 MHz, respectively). Experiments were performed at 30 °C in  $\text{DMSO}-d_6$  or  $\text{acetone}-d_6$ . (The stability of the complex in such media was previously stated.) Heteronuclear correlation experiments (2D-HETCOR), HMQC (multiple quantum) and HMBC (multiple bond), were performed with the same instrument.

**General Procedure for the Preparation of  $[\text{PdCl}_2(\text{HL})]$  Complexes, 9–16.**  $\text{Na}_2[\text{PdCl}_4]$  (100 mg, 0.34 mmol) or  $[\text{Pd}^{\text{II}}\text{Cl}_2(\text{DMSO})_2]$  (100 mg, 0.30 mmol) and the corresponding ligand (0.3–0.4 mmol) were heated under reflux in methanol (10 mL) for 3 h, after which a solid precipitated. The solid was filtered off and washed with hot methanol followed by warm water.

**Complex 9,  $[\text{PdCl}_2(\text{HL1})]$ .** Dark red solid; yield: 80%.  $\lambda_{\text{max}}$  (DMSO) = 430. IR ( $\text{cm}^{-1}$ ):  $\nu(\text{C}=\text{N})$  1582,  $\nu_s(\text{NO}_2)$  1351,  $\nu(\text{C}=\text{S})$  819. Raman ( $\text{cm}^{-1}$ ):  $\nu(\text{C}=\text{N})$  1573. Anal. ( $\text{C}_6\text{H}_6\text{Cl}_2\text{N}_4\text{O}_3\text{SPd}$ ) C, H, N, S.

**Complex 10,  $[\text{PdCl}_2(\text{HL2})]$ .** Orange solid; yield: 88%.  $\lambda_{\text{max}}$  (DMSO) = 424. IR ( $\text{cm}^{-1}$ ):  $\nu(\text{C}=\text{N})$  1595,  $\nu_s(\text{NO}_2)$  1347,  $\nu(\text{C}=\text{S})$  780. Raman ( $\text{cm}^{-1}$ ):  $\nu(\text{C}=\text{N})$  1595. Anal. ( $\text{C}_7\text{H}_8\text{Cl}_2\text{N}_4\text{O}_3\text{SPd}$ ) C, H, N, S.

**Complex 11,  $[\text{PdCl}_2(\text{HL3})]$ .** Orange solid; yield: 70%.  $\lambda_{\text{max}}$  (DMSO) = 430. IR ( $\text{cm}^{-1}$ ):  $\nu(\text{C}=\text{N})$  1554,  $\nu_s(\text{NO}_2)$  1349,  $\nu(\text{C}=\text{S})$  775. Raman ( $\text{cm}^{-1}$ ):  $\nu(\text{C}=\text{N})$  1556. Anal. ( $\text{C}_8\text{H}_{10}\text{Cl}_2\text{N}_4\text{O}_3\text{SPd}$ ) C, H, N, S.

**Complex 12,  $[\text{PdCl}_2(\text{HL4})]$ .** Red brown solid; yield: 50%.  $\lambda_{\text{max}}$  (DMSO) = 434. IR ( $\text{cm}^{-1}$ ):  $\nu(\text{C}=\text{N})$  1604,  $\nu_s(\text{NO}_2)$  1347,  $\nu(\text{C}=\text{S})$  763. Raman ( $\text{cm}^{-1}$ ):  $\nu(\text{C}=\text{N})$  1593. Anal. ( $\text{C}_{12}\text{H}_{10}\text{Cl}_2\text{N}_4\text{O}_3\text{SPd}$ ) C, H, N, S.

**Complex 13,  $[\text{PdCl}_2(\text{HL5})]$ .** Red solid; yield: 40%.  $\lambda_{\text{max}}$  (DMSO) = 338, 455. IR ( $\text{cm}^{-1}$ ):  $\nu(\text{C}=\text{N})$  1578,  $\nu_s(\text{NO}_2)$  1351,  $\nu(\text{C}=\text{S})$  780. Raman ( $\text{cm}^{-1}$ ):  $\nu(\text{C}=\text{N})$  1576. Anal. ( $\text{C}_8\text{H}_8\text{Cl}_2\text{N}_4\text{O}_3\text{SPd}$ ) C, H, N, S.

**Complex 14,  $[\text{PdCl}_2(\text{HL6})]$ .** Brown orange solid; yield: 80%.  $\lambda_{\text{max}}$  (DMSO) = 340, 456. IR ( $\text{cm}^{-1}$ ):  $\nu(\text{C}=\text{N})$  1571,  $\nu_s(\text{NO}_2)$  1348,  $\nu(\text{C}=\text{S})$  788. Raman ( $\text{cm}^{-1}$ ):  $\nu(\text{C}=\text{N})$  1580. Anal. ( $\text{C}_9\text{H}_{10}\text{Cl}_2\text{N}_4\text{O}_3\text{SPd}$ ) C, H, N, S.

**Complex 15,  $[\text{PdCl}_2(\text{HL7})]$ .** Dark red solid; yield: 74%.  $\lambda_{\text{max}}$  (DMSO) = 340, 458. IR ( $\text{cm}^{-1}$ ):  $\nu(\text{C}=\text{N})$  1559,  $\nu_s(\text{NO}_2)$  1352,

$\nu(\text{C}=\text{S})$  783. Raman ( $\text{cm}^{-1}$ ):  $\nu(\text{C}=\text{N})$  1565. Anal. ( $\text{C}_{10}\text{H}_{12}\text{Cl}_2\text{N}_4\text{O}_3\text{SPd}$ ) C, H, N, S.

**Complex 16,  $[\text{PdCl}_2(\text{HL8})]$ .** Dark red solid; yield: 65%.  $\lambda_{\text{max}}$  (DMSO) = 346, 463. IR ( $\text{cm}^{-1}$ ):  $\nu(\text{C}=\text{N})$  1582,  $\nu_s(\text{NO}_2)$  1349,  $\nu(\text{C}=\text{S})$  756. Raman ( $\text{cm}^{-1}$ ):  $\nu(\text{C}=\text{N})$  1568. Anal. ( $\text{C}_{14}\text{H}_{12}\text{Cl}_2\text{N}_4\text{O}_3\text{SPd}$ ) C, H, N, S.

**General Procedure for the Preparation of  $[\text{Pd}(\text{L})_2]$  Complexes, 17–24.**  $\text{Na}_2[\text{PdCl}_4]$  (100 mg, 0.34 mmol) or  $[\text{Pd}^{\text{II}}\text{Cl}_2(\text{DMSO})_2]$  (100 mg, 0.30 mmol) and the corresponding ligand (0.6–0.7 mmol) were heated under reflux in methanol (10 mL) for 3 h, after which a solid precipitated. The solid was filtered off and washed with hot methanol followed by warm water.

**Complex 17,  $[\text{Pd}(\text{L1})_2]$ .** Dark red solid; yield: 83%.  $\lambda_{\text{max}}$  (DMSO) = 434. IR ( $\text{cm}^{-1}$ ):  $\nu(\text{C}=\text{N})$  1577,  $\nu_s(\text{NO}_2)$  1357,  $\nu(\text{C}=\text{S})$  763. Raman ( $\text{cm}^{-1}$ ):  $\nu(\text{C}=\text{N})$  1573. Anal. ( $\text{C}_{12}\text{H}_{10}\text{N}_8\text{O}_6\text{S}_2\text{Pd}$ ) C, H, N, S.  $[\text{Pd}(\text{L1})_2]\cdot\text{DMSO}$  was obtained by slow diffusion of water into a DMSO solution of  $[\text{Pd}(\text{L1})_2]$ . Anal. ( $\text{C}_{14}\text{H}_{16}\text{N}_8\text{O}_7\text{S}_3\text{Pd}$ ) C, H, N, S.

**Complex 18,  $[\text{Pd}(\text{L2})_2]$ .** Brown solid; yield: 90%.  $\lambda_{\text{max}}$  (DMSO) = 416. IR ( $\text{cm}^{-1}$ ):  $\nu(\text{C}=\text{N})$  1579,  $\nu_s(\text{NO}_2)$  1353,  $\nu(\text{C}=\text{S})$  721. Raman ( $\text{cm}^{-1}$ ):  $\nu(\text{C}=\text{N})$  1580. Anal. ( $\text{C}_{14}\text{H}_{14}\text{N}_8\text{O}_6\text{S}_2\text{Pd}$ ) C, H, N, S.

**Complex 19,  $[\text{Pd}(\text{L3})_2]$ .** Orange solid; yield: 75%.  $\lambda_{\text{max}}$  (DMSO) = 424. IR ( $\text{cm}^{-1}$ ):  $\nu(\text{C}=\text{N})$  1578,  $\nu_s(\text{NO}_2)$  1351,  $\nu(\text{C}=\text{S})$  719. Raman ( $\text{cm}^{-1}$ ):  $\nu(\text{C}=\text{N})$  1576. Anal. ( $\text{C}_{16}\text{H}_{18}\text{N}_8\text{O}_6\text{S}_2\text{Pd}$ ) C, H, N, S.

**Complex 20,  $[\text{Pd}(\text{L4})_2]$ .** Orange solid; yield: 65%.  $\lambda_{\text{max}}$  (DMSO) = 436. IR ( $\text{cm}^{-1}$ ):  $\nu(\text{C}=\text{N})$  1560,  $\nu_s(\text{NO}_2)$  1347,  $\nu(\text{C}=\text{S})$  727. Raman ( $\text{cm}^{-1}$ ):  $\nu(\text{C}=\text{N})$  1578. Anal. ( $\text{C}_{24}\text{H}_{18}\text{N}_8\text{O}_6\text{S}_2\text{Pd}$ ) C, H, N, S.

**Complex 21,  $[\text{Pd}(\text{L5})_2]$ .** Red brown solid; yield: 70%.  $\lambda_{\text{max}}$  (DMSO) = 334, 443. IR ( $\text{cm}^{-1}$ ):  $\nu(\text{C}=\text{N})$  1561,  $\nu_s(\text{NO}_2)$  1350,  $\nu(\text{C}=\text{S})$  753. Raman ( $\text{cm}^{-1}$ ):  $\nu(\text{C}=\text{N})$  1563. Anal. ( $\text{C}_{16}\text{H}_{14}\text{N}_8\text{O}_6\text{S}_2\text{Pd}$ ) C, H, N, S.

**Complex 22,  $[\text{Pd}(\text{L6})_2]$ .** Orange solid; yield: 80%.  $\lambda_{\text{max}}$  (DMSO) = 416 nm IR ( $\text{cm}^{-1}$ ):  $\nu(\text{C}=\text{N})$  1596,  $\nu_s(\text{NO}_2)$  1351,  $\nu(\text{C}=\text{S})$  726. Raman ( $\text{cm}^{-1}$ ):  $\nu(\text{C}=\text{N})$  1595. Anal. ( $\text{C}_{18}\text{H}_{18}\text{N}_8\text{O}_6\text{S}_2\text{Pd}$ ) C, H, N, S.

**Complex 23,  $[\text{Pd}(\text{L7})_2]$ .** Red solid; yield: 80%.  $\lambda_{\text{max}}$  (DMSO) = 340, 455. IR ( $\text{cm}^{-1}$ ):  $\nu(\text{C}=\text{N})$  1587,  $\nu_s(\text{NO}_2)$  1349,  $\nu(\text{C}=\text{S})$  748. Raman ( $\text{cm}^{-1}$ ):  $\nu(\text{C}=\text{N})$  1590. Anal. ( $\text{C}_{20}\text{H}_{22}\text{N}_8\text{O}_6\text{S}_2\text{Pd}$ ) C, H, N, S.

**Complex 24,  $[\text{Pd}(\text{L8})_2]$ .** Dark red solid; yield: 78%.  $\lambda_{\text{max}}$  (DMSO) = 351, 471. IR ( $\text{cm}^{-1}$ ):  $\nu(\text{C}=\text{N})$  1570,  $\nu_s(\text{NO}_2)$  1347,  $\nu(\text{C}=\text{S})$  710. Raman ( $\text{cm}^{-1}$ ):  $\nu(\text{C}=\text{N})$  1568. Anal. ( $\text{C}_{28}\text{H}_{22}\text{N}_8\text{O}_6\text{S}_2\text{Pd}$ ) C, H, N, S.  $[\text{Pd}(\text{L8})_2]\cdot 2\text{DMSO}$  was obtained by slow diffusion of water into a DMSO solution of  $[\text{Pd}(\text{L8})_2]$ . Anal. ( $\text{C}_{32}\text{H}_{34}\text{N}_8\text{O}_8\text{S}_4\text{Pd}$ ) C, H, N, S.

**X-ray Diffraction Data and Crystal Structure Determination and Refinement.** Crystallographic data excluding structure factors for the structure reported in this article have been deposited with the Cambridge Crystallographic Data Centre as supplementary publication number CCDC-286670. Copies of data can be obtained, free of charge, upon application to CCDC, 12 Union Road, Cambridge CB2 1EZ, U.K. (Fax: +44-(0)1223-336033; e-mail, deposit@ccdc.cam.ac.uk). The three DMSO solvent molecules showed positional disorder, giving rise to large displacement parameters. The disorder exhibited by one of these molecules was modeled in terms of two positions for the sulfur atom (mirror-related through the plane defined by the oxygen and the two carbon atoms) and refined such as to keep the sum of the occupations equal to zero. The hydrogen atoms of the thiosemicarbazone ligands were included in the molecular model at stereochemical positions and refined with the riding model.

**Biology. In Vitro Biological Evaluation.** The Tulahuen 2 strain stocks of *T. cruzi* were used in this study. Handling of live *T. cruzi* was done according to established guidelines.<sup>44</sup> The epimastigote form of the parasite was grown at 28 °C in an axenic medium (BHI-Tryptose), complemented with 10% fetal calf serum. Cells from a 5 day-old culture were inoculated into 50 mL of fresh culture medium to give an initial concentration of  $1 \times 10^6$  cells/mL. Cell

growth was followed by daily measuring the absorbance of the culture at 600 nm for 11 days. Before inoculation, the media was supplemented with 5  $\mu\text{M}$  of compounds from a stock DMSO solution. The final DMSO concentration in the culture media never exceeded 0.4% (v/v) and had no effect by itself on the proliferation of the parasites (no effect on epimastigote growth was observed by the presence of up to 1% DMSO in the culture media). The compound's ability to inhibit growth of the parasite was evaluated, in triplicate, in comparison to that of the control (no drug added to the media). The control was run in the presence of 0.4% DMSO and in the absence of any drug. The percentage of growth inhibition (PGI) was calculated as follows:  $\text{percentage} = \{1 - [(A_p - A_{0p}) / (A_c - A_{0c})]\} \times 100$ , where  $A_p = A_{600}$  of the culture containing the drug at day 5;  $A_{0p} = A_{600}$  of the culture containing the drug just after the addition of the inocula (day 0);  $A_c = A_{600}$  of the culture in the absence of any drug (control) at day 5;  $A_{0c} = A_{600}$  in the absence of the drug at day 0. Nfx was used as the reference trypanocidal drug, and the activity of compounds was expressed as rPGINfx, ratio of percentage of growth inhibition respect to Nfx taking  $\text{PGINfx} = 1.0$ . The  $\text{IC}_{50}$  (50% inhibitory concentration) was assessed for compounds presenting higher trypanocidal activity than Nfx.<sup>16,45</sup>

**Cyclic Voltammetry Experiments.** DMSO (spectroscopy grade) was used as the solvent and tetrabutylammonium perchlorate (TBAP) as the supporting electrolyte. Cyclic voltammetry was carried out using a Metrohm 693 VA instrument with a 694 VA Stand convertor and a 693 VA Processor in DMSO (ca.  $1.0 \times 10^{-3}$  mol  $\text{L}^{-1}$ ) under a nitrogen atmosphere at room temperature with TBAP (ca. 0.1 mol  $\text{L}^{-1}$ ), using a three-electrode cell. A mercury-dropping electrode was used as the working electrode, a platinum wire as the auxiliary electrode, and saturated calomel as the reference electrode.

**Intracellular Free Radical Production.** The free radical production capacity of the new complexes was assessed in the parasite by Electronic Spin Resonance (ESR) using 5,5-dimethyl-1-pyrroline-*N*-oxide (DMPO) for spin trapping. Each tested compound was dissolved in DMF (spectroscopy grade) (ca. 1 mM), and the solution was added to a mixture containing the epimastigote form of *T. cruzi* (Tulahuen or Brener strains, 4–8 mg/mL protein), 1 mM EDTA, 1 mM NADPH, and 100 mM DMPO in 50 mM phosphate buffer at pH 7.4. The mixture was transferred to a 50  $\mu\text{L}$  capillary. ESR spectra were recorded in the X band (9.85 GHz) using a Bruker ECS 106 spectrometer with a rectangular cavity and 50 kHz field modulation. All of the spectra were registered in the same scale after 15 scans.

**Oxygen Uptake.** Tulahuen strain *T. cruzi* epimastigotes were harvested by 500g centrifugation, followed by washing and re-suspension in 0.05 M sodium phosphate buffer at pH 7.4 and containing 0.107 M sodium chloride. Respiration measurements were carried out polarographically with a Clark electrode (Yellow Springs Instruments, 53 YSI model).<sup>46</sup> The chamber volume was 2 mL, and the temperature was 28 °C. The amount of parasite used was equivalent to 1.2 mg of protein/mL. To evaluate redox cycling, the mitochondrial respiration was inhibited with 0.3 mM sodium cyanide. The  $\text{IC}_{50}$  equivalent concentration corresponds to the final concentration used in the oxygen uptake experiments. This concentration was calculated considering that the  $\text{IC}_{50}$  (culture growth experiments) was determined using  $3 \times 10^6$  parasites/mL, equivalent to 0.0375 mg protein/mL as initial parasite mass;  $80 \times 10^6$  parasites/mL, equivalent to 1 mg protein/mL, was used in the oxygen uptake experiments. To maintain the parasite mass-to-drug ratio constant in these two types of experiments, the original  $\text{IC}_{50}$  was corrected by this 26-fold parasite mass increase in the oxygen uptake experiments. The results were corrected according to the observed effect produced by DMSO alone.

***T. cruzi* Trypanothione Reductase (TR) Inhibition Assays.** Recombinant *T. cruzi* TR was prepared according to a published procedure.<sup>47</sup> Trypanothione disulfide was purchased from Bachem, Heidelberg, Germany.

TR activity was measured spectrophotometrically at 25 °C in a TR assay buffer (40 mM Hepes, 1 mM EDTA, pH 7.5) as

described.<sup>48</sup> Stock solutions of the complexes **9**, **13**, **15**, and **23** and the free ligand **7** were prepared in DMSO. The assay mixtures (1 mL) were contained in a TR assay buffer, 100  $\mu\text{M}$  NADPH, and 105 or 93  $\mu\text{M}$  trypanothione disulfide ( $\text{TS}_2$ ), and varying concentrations of the inhibitor. NADPH, enzyme, and inhibitor were mixed, and the reaction was started by adding  $\text{TS}_2$ . The absorption decrease at 340 nm due to NADPH consumption was followed. Control assays contained the respective amount of DMSO instead of the inhibitor.

**Test of Irreversible Inhibition of TR.** To monitor the time-dependent inactivation, 425 mU of TR in a total volume of 100  $\mu\text{L}$  was incubated at 25 °C with 12–120  $\mu\text{M}$  inhibitor in the presence of 200  $\mu\text{M}$  NADPH. At different time intervals (0–150 min), 5  $\mu\text{L}$  aliquots were removed, and the remaining activity was measured in a standard TR assay. Because of the dilution, reversible inhibition is not recorded under these conditions. The residual solutions were dialyzed overnight, and the activity was again determined by adding an aliquot, with and without previous treatment with excess thiol, in a standard TR assay. Two control series contained buffer, TR, and NADPH or buffer, TR, and inhibitor.

**Calf Thymus DNA Interaction Experiments.** The complexes were tested for their DNA interaction ability using native calf thymus DNA, CT DNA, (type I) by a modification of a previously reported procedure.<sup>49</sup> CT DNA (50 mg) was dissolved in water (30 mL) (overnight), and the concentration per nucleotide was determined by UV absorption spectroscopy using the molar absorption coefficient of 6000 mol<sup>-1</sup>dm<sup>3</sup>cm<sup>-1</sup> at 260 nm. The solutions of the complexes in DMSO (spectroscopy grade) (1 mL, 10<sup>-3</sup> M) were incubated at 37 °C with solution of CT DNA (1 mL) during 96 h. DNA/complex mixtures were exhaustively washed to eliminate the unreacted complex. Quantification of bound palladium was done by atomic absorption spectroscopy on a Perkin-Elmer 380 spectrometer. Standards were prepared by diluting a palladium standard solution. Interaction levels were determined as nmol of Pd bound per mg of DNA base or as mol of Pd bound per mol of DNA base.

**Acknowledgment.** This work was supported by CSIC (Project 297/04, UdelaR), FCE 10002, and PEDECIBA of Uruguay, TWAS (RGA 02-036 and RGA 04- 205), FAPESP of Brazil, FONDECYT 1030949 and "Proyecto Anillo en Ciencia y Tecnología, Bicentenario/CONICYT" from Chile, and CONICET of Argentina as well as by the Deutsche Forschungsgemeinschaft (SFB 544 Control of Tropical Infectious Diseases to R.L.K.-S.). L.O. thanks RTPD (Research and Training in Parasitic Diseases network)-SIDA/SAREC for financing a research visit to Chile. Edith Röckel is acknowledged for the kinetic analysis of trypanothione reductase.

**Supporting Information Available:** Crystal data, data collection procedure, structure determination methods, refinement results, and microanalytical results. This material is available free of charge via the Internet at <http://pubs.acs.org>.

## References

- 1) <http://www.who.int/ctd/chagas>.
- 2) Urbina, J. New chemotherapeutic approaches for the treatment of Chagas disease. *Expert. Opin. Ther. Patents* **2003**, *13*, 661–669.
- 3) Cerecetto, H.; González, M. Chemotherapy of Chagas disease: status and new developments. *Curr. Top. Med. Chem.* **2002**, *2*, 1185–1190.
- 4) Zhang, C.; Lippard, S. New metal complexes as potential therapeutics. *Curr. Opin. Chem. Biol.* **2003**, *7*, 481–489.
- 5) Farrell, N. Metal complexes as drugs and chemotherapeutic agents. *Compr. Coord. Chem. II* **2003**, *9*, 809–840.
- 6) Sánchez-Delgado, R. A.; Anzellotti, A.; Suárez, L. Metal complexes as chemotherapeutic agents against tropical diseases: malaria, trypanosomiasis, and leishmaniasis. *Metal Ions in Biological Systems*; Marcel Dekker: New York, 2004; Vol. 41, pp 379–419.
- 7) Sánchez-Delgado, R. A.; Anzellotti, A. Metal complexes as chemotherapeutic agents against tropical diseases: trypanosomiasis, malaria and leishmaniasis. *Mini-Rev. Med. Chem.* **2004**, *4*, 23–30.



- (8) Sánchez-Delgado, R. A.; Lazard, K.; Rincon, L.; Urbina, J. A. Towards a novel metal-based chemotherapy against tropical diseases. 1. Enhancement of the efficacy of clotrimazole against *Trypanosoma cruzi* by complexation to ruthenium in RuCl<sub>2</sub>(clotrimazole). *J. Med. Chem.* **1993**, *36*, 2041–2043.
- (9) Sánchez-Delgado, R. A.; Navarro, M.; Lazard, K.; Atencio, R.; Caparelli, M.; Vargas, F.; Urbina, J.; Boulliez, A.; Noels, A.; Masi, D. Toward a novel metal-based chemotherapy against tropical diseases. 4. Synthesis and characterization of new metal-clotrimazole complexes and evaluation of their activity against *Trypanosoma cruzi*. *Inorg. Chim. Acta* **1998**, *275–276*, 528–540.
- (10) Navarro, M.; Lehman, T.; Cisneros-Fajardo, E.; Fuentes, A.; Sánchez Delgado, R.; Urbina, J. Toward a novel metal-based chemotherapy against tropical diseases. 5. Synthesis and characterization of new Ru(II) and Ru(III) clotrimazole and ketoconazole complexes and evaluation of their activity against *Trypanosoma cruzi*. *Polyhedron* **2000**, *19*, 2319–2325.
- (11) Navarro, M.; Cisneros-Fajardo, E. J.; Lehmann, T.; Sanchez-Delgado, R. A.; Atencio, R.; Silva, P.; Lira, R.; Urbina, J. A. Toward a novel metal-based chemotherapy against tropical diseases. 6. Synthesis and characterization of new copper(II) and gold(I) clotrimazole and ketoconazole complexes and evaluation of their activity against *Trypanosoma cruzi*. *Inorg. Chim. Acta* **2001**, *40*, 6879–6884.
- (12) Chibale, K. Towards broad spectrum antiprotozoal agents. *ARKIVOC* **2002**, *IX*, 93–98.
- (13) Farrell, N. P. In *Catalysis by Metal Complexes*; James, B. R., Ugo, R., Eds.; Reidel-Kluwer Academic Press: Dordrecht, Holland, 1989.
- (14) Gómez-Quiroga, A.; Navarro-Ranninger, C. Contribution to the SAR field of metalated and coordination complexes. Studies of the palladium and platinum derivatives with selected thiosemicarbazones as antitumoral drugs. *Coord. Chem. Rev.* **2004**, *248*, 119–133.
- (15) Moreno, S. N.; Mason, R.; Docampo, R. Reduction of nifurtimox and nitrofurantoin to free radical metabolites by rat liver mitochondria. Evidence of an outer membrane-located nitroreductase. *J. Biol. Chem.* **1984**, *259*, 298–305.
- (16) Aguirre, G.; Cerecetto, H.; González, M.; Gambino, D.; Otero, L.; Olea-Azar, C.; Rigol, C.; Denicola, A. In vitro activity and mechanism of action against the protozoan parasite *Trypanosoma cruzi* of 5-nitrofuril containing thiosemicarbazones. *Bioorg. Med. Chem.* **2004**, *12*, 4885–4893.
- (17) Henderson, G. B.; Ulrich, P.; Fairlamb, A. H.; Rosenberg, I.; Pereira, M.; Sela, M.; Cerami, A. "Subversive" substrates for the enzyme trypanothione disulfide reductase: alternative approach to chemotherapy of Chagas disease. *Proc. Natl. Acad. Sci. U.S.A.* **1988**, *85*, 5374–5378.
- (18) Croft, S. L. Pharmacological approaches to antitrypanosomal chemotherapy. *Mem. Inst. Oswaldo Cruz* **1999**, *94*, 215–220.
- (19) (a) Bonse, S.; Richards, J. M.; Ross, S. A.; Lowe, G.; Krauth-Siegel, R. L. (2,2':6',2''-Terpyridine)platinum(II) complexes are irreversible inhibitors of *Trypanosoma cruzi* trypanothione reductase but not of human glutathione reductase. *J. Med. Chem.* **2000**, *43*, 4812–4821. (b) Lowe, G.; Droz, A. S.; Vilaiyan, T.; Weaver, G. W.; Tweedale, L.; Pratt, J. M.; Rock, P.; Yardley, V.; Croft, S. L. Cytotoxicity of (2,2':6',2''-terpyridine)platinum(II) complexes to *Leishmania donovani*, *Trypanosoma cruzi*, and *Trypanosoma brucei*. *J. Med. Chem.* **1999**, *42*, 999–1006.
- (20) Schmidt, A.; Krauth-Siegel, R. L. Enzymes of the trypanothione metabolism as targets for antitrypanosomal drug development. *Curr. Top. Med. Chem.* **2002**, *2*, 1239–1259.
- (21) Meiering, S.; Inhoff, O.; Mies, J.; Vincek, A.; Garcia, G.; Kramer, B.; Dormeyer, M.; Krauth-Siegel, R. L. Inhibitors of *Trypanosoma cruzi* trypanothione reductase revealed by virtual screening and parallel synthesis. *J. Med. Chem.* **2005**, *48*, 4793–4802.
- (22) Inhoff, O.; Richards, J. M.; Briet, J. W.; Lowe, G.; Krauth-Siegel, R. L. Coupling of a competitive and an irreversible ligand generates mixed type inhibitors of *Trypanosoma cruzi* trypanothione reductase. *J. Med. Chem.* **2002**, *45*, 4524–4530.
- (23) Kovala-Demertzi, D.; Domopoulou, A.; Demertzis, M. A.; Valle, G.; Papageorgiou, A. Palladium(II) complexes of 2-acetylpyridine N(4)-methyl, N(4)-ethyl and N(4)-phenyl-thiosemicarbazones. Crystal structure of chloro(2-acetylpyridine N(4)-methylthiosemicarbazato) Palladium(II). Synthesis, spectral studies, in vitro and in vivo antitumour activity. *J. Inorg. Biochem.* **1997**, *68*, 147–155.
- (24) Fostiak, L. M.; Garcia, M. I.; Swearingen, J. K.; Bermejo, E.; Castiñeiras, A.; West, D. X. Structural and spectral characterization of transition metal complexes of 2-pyridineformamide N(4)-dimethylthiosemicarbazone. *Polyhedron* **2003**, *22*, 83–92.
- (25) Afrasiabi, Z.; Sinn, E.; Chen, J.; Ma, Y.; Rheingold, A. L.; Zakharov, L. N.; Rath, N.; Padhye, S. Appended 1,2-naphthoquinones as anticancer agents 1: Synthesis, structural, spectral and antitumor activities of *ortho*-naphthoquinone thiosemicarbazone and its transition metal complexes. *Inorg. Chim. Acta* **2004**, *357*, 271–278.
- (26) Kovala-Demertzi, D.; Domopoulou, A.; Demertzis, M. A.; Raptopoulou, C. P.; Terzis, A. Coordination properties of 2-acetylpyridine thiosemicarbazone. Palladium(II) complexes with neutral and deprotonated ligand. X-ray structure of bromo(2-acetylpyridine Thiosemicarbazonato) palladium(II). *Polyhedron* **1994**, *13*, 1917–1925.
- (27) Kovala-Demertzi, D.; Miller, J. R.; Kourkoumelis, N.; Hadjikou, S. K.; Demertzis, M. A. Palladium(II) and platinum(II) complexes of pyridine-2-carboxaldehyde thiosemicarbazone with potential biological activity. Synthesis, structure and spectral properties. Extended network via hydrogen linkages of [Pd(PyTsc)Cl]. *Polyhedron* **1999**, *18*, 1005–1009.
- (28) Johnson, C. K. Report ORNL-5138; Oak Ridge National Laboratory, Oak Ridge, TN, 1976.
- (29) Kovala-Demertzi, D.; Demertzis, M. A.; Castiñeiras, A.; West, D. Palladium(II) complexes of 2-acetyl- and 2-formylpyridine 3-hexamethyleneimanyl-thiosemicarbazones: A synthetic, spectral and structural study. *Polyhedron* **1998**, *17*, 3739–3745.
- (30) Papathanasis, L.; Demertzis, M. A.; Yadav, P. N.; Kovala-Demertzi, D.; Prentjas, C.; Castiñeiras, A.; Skoulika, S.; West, D. X. Palladium(II) and platinum(II) complexes of 2-hydroxy acetophenone N(4)-ethylthiosemicarbazone -crystal structure and description of bonding properties. *Inorg. Chim. Acta* **2004**, *357*, 4113–4120.
- (31) Nath-Yadav, P.; Demertzis, M.; Kovala-Demertzi, D.; Skoulika, S.; West, D. W. Palladium(II) complexes of 4-formylantipyrene N(3)-substituted thiosemicarbazones: first example of X-ray crystal structure and description of bonding properties. *Inorg. Chim. Acta* **2003**, *349*, 30–36.
- (32) Vila, J. M.; Pereira, T.; Amoedo, A.; Graña, M.; Martínez, J.; López-Torres, M.; Fernández, A. The key role of sulfur in thiosemicarbazone compounds. Crystal and molecular structure of [Pd(4-MeOC<sub>6</sub>H<sub>4</sub>C(Me)=NN=C(S)NPh)<sub>2</sub>]. *J. Organomet. Chem.* **2001**, *623*, 176–184.
- (33) (a) Otero, L.; Noblia, P.; Gambino, D.; Cerecetto, H.; González, M.; Di Maio, R.; Ellena, J.; Piro, O. E. Synthesis and characterization of new ruthenium complexes with active ligands against Chagas' Disease. *Inorg. Chim. Acta* **2003**, *344*, 85–94. (b) Otero, L.; Noblia, P.; Gambino, D.; Cerecetto, H.; González, M.; Sánchez Delgado, R.; Castellano, E. E.; Piro, O. E. New Re(V) nitrofuril semicarbazone complexes. Crystal structure of [ReOCl<sub>2</sub>(PPh<sub>3</sub>)(3-(5-nitrofuril)-acroleine semicarbazone)]. *Z. Anorg. Allg. Chem.* **2003**, *629*, 1033–1038. (c) Casas, S.; García-Tasende, M. S.; Sordo, J. Main group metal complexes of semicarbazones and thiosemicarbazones. A structural review. *Coord. Chem. Rev.* **2000**, *209*, 197–261.
- (34) Rigol, C.; Olea-Azar, C.; Mendizábal, F.; Otero, L.; Gambino, D.; González, M.; Cerecetto, H. Electrochemical and ESR study of 5-nitrofuril-containing thiosemicarbazones antiprotozoal drugs. *Spectrochim. Acta, Part A* **2005**, *61*, 2933–2938.
- (35) Olea-Azar, C.; Rigol, C.; Opazo, L.; Morello, A.; Maya, J. D.; Repetto, Y.; Aguirre, G.; Cerecetto, H.; Di Maio, R.; González, M.; Porcal, W. ESR and spin trapping studies of two new potential antitrypanosomal drugs. *J. Chil. Chem. Soc.* **2003**, *48*, 65–67.
- (36) Olea-Azar, C.; Rigol, C.; Mendizábal, F.; Morello, A.; Maya, J. D.; Moncada, C.; Cabrera, E.; Di Maio, R.; González, M.; Cerecetto, H. ESR spin trapping studies of free radicals generated from nitrofuril derivative analogues of Nifurtimox by electrochemical and *Trypanosoma cruzi* reduction. *Free Radical Res.* **2003**, *37*, 993–1001.
- (37) Makino, K.; Hagiwara, T.; Murakami, A. A mini review: fundamental aspects of spin trapping with DMPO. *Radiat. Phys. Chem.* **1991**, *37*, 657–665.
- (38) Sinha, B. K. Free radicals in anticancer drug pharmacology. *Chem.-Biol. Interact.* **1989**, *69*, 293–317.
- (39) Hawkins, C. L.; Davies, M. J. Hypochlorite-induced damage to nucleosides: formation of chloramines and nitrogen-centered radicals. *Chem. Res. Toxicol.* **2001**, *14*, 1071–1081.
- (40) Maya, J. D.; Bollo, S.; Nuñez-Vergara, L. J.; Squella, J. A.; Repetto, Y.; Morello, A.; Périé, J.; Chauvière, G. *Trypanosoma cruzi*: effect and mode of action of nitroimidazole and nitrofuril derivatives. *Biochem. Pharmacol.* **2003**, *65*, 999–1006.
- (41) Brabec, V. DNA modifications by antitumor platinum and ruthenium compounds: their recognition and repair. *Progress in Nucleic Acid Research and Molecular Biology*; Elsevier Science: USA, 2002; Vol. 71, pp 1–68.
- (42) Price, J. H.; Williamson, A. N.; Shramm, R. F.; Wayland, B. B. Palladium(II) and platinum(II) alkyl sulfoxide complexes. Examples of sulfur-bonded, mixed sulfur- and oxygen-bonded, and totally oxygen bonded complexes. *Inorg. Chem.* **1972**, *11*, 1280–1284.
- (43) Geary, W. J. The use on conductivity measurements in organic solvents for the characterization of coordination compounds. *Coord. Chem. Rev.* **1971**, *7*, 81–91.
- (44) Huang, L.; Lee, A.; Ellman, J. A. Identification of potent and selective mechanism-based inhibitors of the cysteine protease cruzain using solid-phase parallel synthesis. *J. Med. Chem.* **2002**, *45*, 676–684.

- (45) Cerecetto, H.; Di Maio, R.; González, M.; Risso, M.; Saenz, P.; Seoane, G.; Denicola, A.; Peluffo, G.; Quijano, C.; Olea-Azar, C. 1,2,5-Oxadiazole *N*-oxide derivatives and related compounds as potential antitrypanosomal drugs. Structure–activity relationships. *J. Med. Chem.* **1999**, *42*, 1941–1950.
- (46) Letelier, M. E.; Rodríguez, E.; Wallace, A.; Lorca, M.; Repetto, Y.; Morello, A.; Aldunate, J. *Trypanosoma cruzi*: a possible control of transfusion induced Chagas disease by phenolic antioxidants. *Exp. Parasitol.* **1990**, *71*, 357–363.
- (47) Sullivan, F. X.; Walsh, C. T. Cloning, sequencing, overproduction and purification of trypanothione reductase from *Trypanosoma cruzi*. *Mol. Biochem. Parasitol.* **1991**, *44*, 145–147.
- (48) Jockers-Scherübl, M. C.; Schirmer, R. H.; Krauth-Siegel, R. L. Trypanothione reductase from *Trypanosoma cruzi*. Catalytic properties of the enzyme and inhibition studies with trypanocidal compounds. *Eur. J. Biochem.* **1989**, *180*, 267–272.
- (49) Mahnken, R. E.; Billadeau, M. A.; Nikonowicz, E. P.; Morrison, H. Towards the development of photo cis-platinum reagents. Reaction of cis-dichlorobis(1, 10-phenanthroline)rhodium(III) with calf thymus DNA, nucleotides and nucleosides. *J. Am. Chem. Soc.* **1992**, *114*, 9253–9265.

JM0512241